Contents lists available at SciVerse ScienceDirect

Optics Communications

journal homepage: www.elsevier.com/locate/optcom

SPP tomography experiments with surface plasmon polariton standing waves

L. Grave de Peralta *, D. Domínguez

Department of Physics, Texas Tech University, Lubbock, TX 79409, USA

ARTICLE INFO

ABSTRACT

Surface plasmon polariton (SPP) standing waves were observed using SPP tomography. We show that SPP tomography in a quantum eraser arrangement has the remarkable capability of permitting the observation of light passing through the dark fringes of the observed standing wave interference pattern. Classical and phenomenological quantum descriptions of the experiments are presented. The experimental results are discussed in the broader context of novel active magnetic–optical metamaterials and the use of electromagnetic standing waves to study magnetic properties of materials at optical frequencies.

© 2012 Elsevier B.V. All rights reserved.

1. introduction

Surface plasmon polaritons (SPPs) have numerous applications based on their sub-wavelength capabilities [1–3]. SPPs are electromagnetic waves (light) coupled to collective oscillations of free electrons which are confined at the interface between a metal and a dielectric [4]. The intrinsic quasi two-dimensional (2D) nature of SPPs has motivated fundamental studies in 2D light propagation, interference, and diffraction phenomena which are highly needed for design and simulation of SPP-based devices. SPP tomography [5–8], also called leakage radiation microscopy [9,10], is a fascinating far-field, non-disturbing, imaging technique that permits reliable investigation of the interference features formed at the metal–air interface of a sample due to the superposition of SPP beams [10–14]. In this work, SPP tomography was used to study the formation of a SPP standing wave due to the superposition of two SPPs traveling in opposite directions in a dielectric loaded SPP waveguide (DLSPPW) [15,16]. The occurrence of the SPP standing wave resulted in the formation of an interference pattern in the DLSPPW with well-defined interference fringes. As in any standing wave, the presence of dark fringes in the observed interference pattern indicates that the net energy flow inside of the waveguide was zero [17,18]. This is because each light beam propagating in opposite direction carries equal

amount of energy. In this work we demonstrate, for the first time, that SPP tomography has the unique capability of permitting detection of light that passes through the dark fringes of a standing wave interference pattern. A comprehensive explanation of this remarkable property is presented. In addition, we discuss the experimental results presented here in the broader context of novel active magnetic optical metamaterials [19,20] and the use of electromagnetic standing waves for studying magnetic properties of materials at optical frequencies [21–23].

We also present a phenomenological quantum description of the formation of an electromagnetic standing wave with relatively intense light, which is in correspondence with the SPP tomography experiments described here. In these measurements, single photon events were not recorded, nor was a source of single photons used; however, it is interesting to analyze the experimental results while focusing on the quantum nature of light. It is reasonable to attempt this analysis because, according to Bohr's correspondence principle [24], classical optics should be an extreme instance of the more precise quantum description of light. A full quantum electrodynamics description [25,26] would be unnecessarily complicated. Instead, we present a phenomenological, but rigorous, quantum description based on the use of the simplest of the three common interpretations of the photon [27], that is, a photon is what produces a "click" in a photodetector. In addition, Feynman's description of interference was used, i.e., the probability of an event is given by $p = |\Phi|^2$, where Φ is a complex number which is called probability amplitude [28]. These basic ideas were chosen because this methodology allows

---

* Corresponding author. Tel.: +1 806 252 6258.
E-mail address: luis.grave-de-peralta@ttu.edu (L. Grave de Peralta).

one to explore the classical limit of the quantum theory without more mathematical or conceptual complexities than that required by a classical description. Nevertheless, this basic phenomenological approach provides a simple method for obtaining the classical limit of the analytical expression of the transversal wavefunction of the photons in an electromagnetic standing wave. In turn, the analytical expression illustrates directly that, in the classical limit, there is a simple relationship between the quantum mechanical probability wave and the electric and magnetic fields of the standing wave. This is an especially useful result for optics engineers and scientists that have not been fully trained in the intricateness of quantum optics.

This paper is organized as follows: In Section 2 the experimental setup used in this work is described and the experimental results are presented. Section 3 is dedicated to a classical discussion of the experiments. A phenomenological quantum description of the formation of an electromagnetic standing wave, which is compatible with the experimental results, is presented in Section 4. Finally, the conclusions of this work are given in Section 5.

2. Experimental results

The SPP tomography arrangement used in the experiments discussed in this work has been described in [5,6]. Briefly, the excitation source was provided by a 10 mW He–Ne laser ($\lambda = 632.8$ nm). The laser beam was equally divided by a cube beam splitter, and then the beams were deflected by mirrors toward a low numerical aperture (NA=0.65, 40 ×) microscope objective lens with slightly different angles. The lens focused the beams into spots of ~5 μm in diameter at the surface of the sample. Fig. 1(a) shows a schematic of the samples used in the experiments. The samples were fabricated by depositing a 1 nm thick chromium adhesion layer on a glass substrate, followed by a 50 nm thick layer of gold. The gold layer was then covered with a 150 nm thick PolyMethylMethAcrylate (PMMA) layer. As sketched in Fig. 1(a), a 25 μm long, single mode DLSPPW with a width of 600 nm was defined onto the PMMA layer by e-beam lithography [16]. Two laser spots were focused at the opposite edges of the waveguide. As sketched in Fig. 1(b), SPPs were excited by scattering and two guided light beams propagated within the waveguide toward each other. The radiation that leaked to the substrate was collected by an immersion oil objective lens (NA=1.49, 100 ×). A set of lenses, internal to the

microscope, perform magnification and aberration correction along with image formation. A charge coupled device (CCD) camera captures the image of the sample surface emission (SE) after being partially reflected by a beam splitter. A second CCD camera collects the image formed in the back focal plane (BFP) of the objective. The BFP image corresponds to the Fourier plane (FP), with respect to the sample surface emission, and is thus a map of the two-dimensional momentum distribution of the SPPs excited in the plane of the sample [5,6,7,13]. Several accessories (spatial filters, a linear polarizer, and a half-wave plate) can be optionally inserted after the high numerical aperture objective lens. These external modifications provide a great deal of flexibility to the SPP tomography arrangement.

Fig. 2(a) and (b) show SE and FP images, respectively, corresponding to a single SPP excited at the left extreme of the DLSPPW. Clear SPP propagation, from the left to the right, in the DLSPPW can be observed in Fig. 2(a). In good correspondence with previous results [16], a propagation length of ~12 μm was estimated from a line profile (not shown here) along the SPP path. The central bright spot shown in Fig. 2(b) is due to the direct transmission of the laser through the sample. The straight vertical segment at the right extreme of the FP image is the signature of a SPP traveling from left to right in the single mode DLSPPW [5,6,13,15]. Additional arc-traces correspond to SPPs excited at the gold–air interface of the sample. The ratio of the distances of
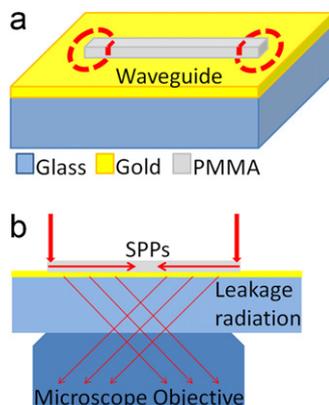

Fig. 1. Sketch of the (a) fabricated DLSPPW and (b) leakage radiation collection optics. The discontinuous circles illustrate the position of the laser spots used to excite SPPs by scattering at the extremes of the waveguide. The light that leaks along the paths of excited SPPs is collected by microscope's immersion oil objective lens.
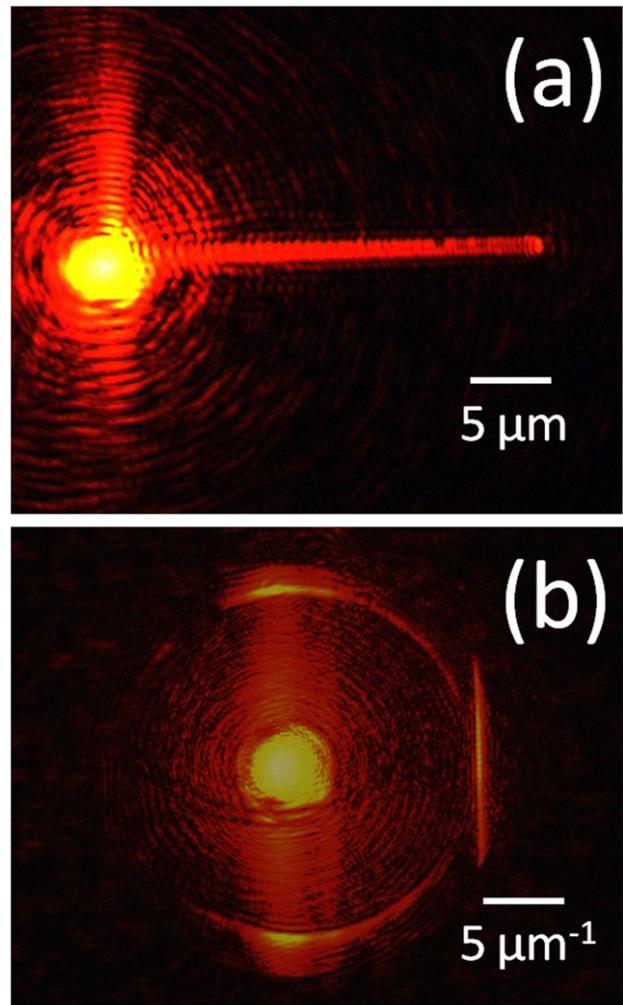

Fig. 2. (a) SE and (b) FP images corresponding to a single SPP exited at the left extreme of the DLSPPW. The straight vertical segment at the right extreme of the FP image is the signature of a SPP traveling from left to right in the waveguide.

the traces to the central spot is equal to the ratio of the corresponding effective refractive indexes (n_{eff}) of the excited SPPs [7]. Therefore, using the reported value of $n_{eff}{\sim}1.03$ for the SPP excited in the gold–air interface [12], we determined $n_{eff}{\sim}1.1$ for the DLSPPW mode. Thus, the wavelength of the SPP excited in the waveguide is $\lambda_{SPP}=\lambda/n_{eff}{\sim}577$ nm.

Fig. 3 shows SE images corresponding to two SPPs excited simultaneously in the DLSPPW. This was confirmed by the presence of two straight-line segments at the right and left extremes of the corresponding FP image (not shown). The leakage radiation associated with each SPP beam has the same polarization state because the excited SPPs propagate in opposite directions [29]. This was confirmed by inserting a linear polarizer in the optical path of the leakage radiation, orienting it such that the transmission axis was aligned to the polarization of the leaked light, and looking at the resulting SE image shown in Fig. 3. In addition, a spatial filter was used to eliminate the direct laser beam and the SPPs excited at the gold–air interface from the SE images shown in Fig. 3. Both linear polarizer and spatial filter were inserted right after the high numerical aperture objective lens as described in [5,6,12,13,29]. Interference fringes separated a distance of${\sim}286$ nm can be seen in the inset of the SE image shown in Fig. 3(a). The observed fringes correspond to the formation of a standing wave in the waveguide. Due to the propagation losses, the fringes are better defined close to the longitudinal center of the waveguide where the intensities of the SPPs propagating in opposite direction are approximately equal. The distance between consecutive bright fringes is equal to half of the wavelength of the wave propagating in the DLSPPW [30]. From this we determined a value of $\lambda_{SPP}{\sim}572$ nm in excellent correspondence with the value determined from the FP image shown in Fig. 2(b).
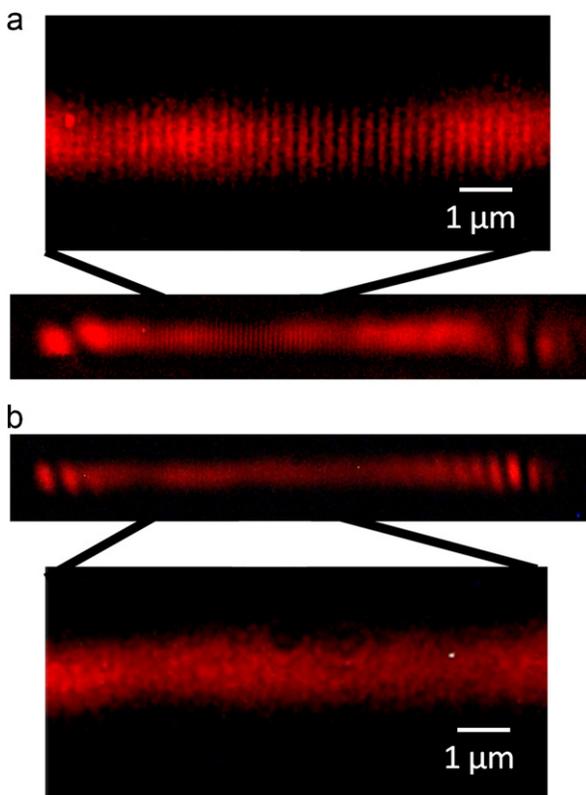

Fig. 3. SE images corresponding to two SPPs exited simultaneously in the DLSPPW. The images were obtained (a) without and (b) with a half-wave plate inserted after the high NA objective lens.

A quantum eraser [12,31] arrangement was formed by introducing a half wave plate, at the BFP of the high NA objective lens and after the linear polarizer, in the optical path of the leakage radiation associated with only one of the excited SPPs. This can easily be done because, at the BFP, the signature features [see straight vertical segment in Fig. 2(b)] of the two excited SPPs are spatially well separated. Therefore, rotation of the half-wave plate resulted in changing the polarization orientation of the leakage radiation associated with only one of the SPPs. Consequently, the interference fringes observed in Fig. 3(a) can disappear and reappear by rotating the half wave plate. From a quantum mechanics point of view, the erasure of the interference fringes occurs because the half wave plate permits the identification of the optical path of the photons by labeling their states of polarization [12,31]. Fig. 3(b) shows an SE image obtained when the half-wave plate was oriented such that the polarizations of the leakage radiation associated with both SPPs excited in the waveguide were orthogonal. As shown in inset of Fig. 3(b), this resulted in the erasure of the interferences fringes from the SE image.

3. Classical discussion of the experimental results

The formation of the standing wave in the DLSPPW can be understood by considering that the electric field distribution near the center of the waveguide is similar to the electric field distribution of a superposition of two plane waves propagating in opposite directions along the z-axis. This has been previously discussed in several optics textbooks [17,30]. For such an analogy, it is also beneficial to assume that, in first approximation, the SPP propagation losses are small. In this approximation the electric and magnetic field distribution in the interference pattern corresponding to the standing wave are described by the following expressions [30]:

$$E_T(z,t)=E(z)\cos(\omega t), E(z)=2E_o\sin(kz) \tag{1}$$

$$B_T(z,t)=B(z)\sin(\omega t), B(z)=-2B_o\cos(kz) \tag{2}$$

where E_o and B_o are the amplitudes of the electric and magnetic fields of both waves respectively, $k=2\pi/\lambda_{SPP}$, and $\omega=2\pi c/\lambda$ with c being the speed of the light. It follows from expressions (1) and (2) that the nodes of E_T occur at the antinodes of B_T and vice versa [17,21–23,30]. This brings attention to an interesting issue: why is light not commonly detected at the nodes of the electric field in a standing wave? The reason for this is well known: common photodetectors are only responsive to the electric field [17,30]. Nevertheless, Fig. 3(b) demonstrates that light passing through the nodes of a standing wave can be detected by SPP tomography in a quantum eraser arrangement. In general, SE images are maps indicating the regions of the gold layer where radiation leaked from, and FP images are maps of the leakage radiation emission direction [5,6]. Fig. 3(a) shows a useful exception of this rule. The presence of dark fringes in Fig. 3(a) does not mean that there is no leakage radiation from the corresponding points in the gold layer. The veracity of this statement is corroborated by the absence of dark fringes in Fig. 3(b), which indicates that light leaks from the gold layer regions where the nodes of the standing wave were formed. Rotation of the half-wave plate, resulting in the apparition of the interference fringes in the SE image, cannot change the starting points of the emitted leakage radiation on the gold layer. The dark fringes seen in Fig. 3(a) are thus the result of the superposition at the CCD camera of the light leaked in opposite directions from the nodes of the standing wave. Therefore, the SE image shown in Fig. 3(b) is a reliable map of the points on the sample surface where the leakage radiation came from.

Consequently, the setup used to obtain Fig. 3(b) permits the detection of light, propagating in opposite directions, through the nodes of the standing wave formed in the DLSPPW. In contrast with the SE image shown in Fig. 3(b), the SE image shown in Fig. 3(a) is an incorrect map of the points of the sample surface that leaked light, but permits observation at the far-field of the standing wave formed in the waveguide [12]. It is worth noting that the formation of a standing wave due to the superposition of SPPs traveling in opposite direction has also been observed using near-field optical techniques [32,33]. However, this is the first time that the uniform illumination shown in Fig. 3(b) has been experimentally observed.

Using expression (1), the intensity of the standing wave in the center of the DLSPPW can be approximately described by the following expression [18,30]:

$$I(z) = 2\alpha_E^2 E^2(z) = 4I_o \sin^2(kz) \tag{3}$$

where I_o is the intensity of each one of the two waves from which superposition results in the standing wave, i.e. [18,30]

$$I_o = 2\alpha_E^2 E_o^2, \alpha_E = \sqrt{\frac{1}{4}c\varepsilon} \tag{4}$$

Here, ε is the effective electrical permittivity of the propagation medium. $I(z)$ corresponds to the interference pattern shown in Fig. 3(a). Intensity minima, $I(z)=0$, occur at the dark fringes of the pattern. Intensity maxima, $I(z)=4I_o$, occur at the bright fringes observed in Fig. 3(a). It is worth noting that $I(z)$ is the intensity that a common photodetector would measure since photodetectors are only responsive to the electric field [34]. For instance, a detector able to measure $I(z)$ may be realized by making the DLSPPW with an adequate photoresist. In fact, the invention of color photography was based on recording the intensity of an electromagnetic standing wave with a photoresist material [17,30]. Nevertheless, recent advances in active magnetic optical metamaterials [19,20] permits one to foresee the future realization of advanced optical photodetectors equally responsive to both electric and magnetic fields. Such advanced photodetectors would measure the presence of light wherever the electric or the magnetic field of the standing wave is not identically zero [21–23]. Therefore, if an advanced photodetector (equally responsive to both electric and magnetic fields) were used to measure the intensity of an electromagnetic standing wave, it would measure the constant intensity, I_g, given by the following expression [18,30]:

$$I_g = \alpha_E^2 E^2(z) + \alpha_B^2 B^2(z) = 2I_o, \alpha_B = \sqrt{\frac{1}{4}\frac{c}{\mu}} \tag{5}$$

where μ is the effective magnetic permeability of the propagation medium. Therefore, such advanced photodetector would not detect the formation of a standing wave interference pattern. This analysis is in excellent correspondence with the uniform intensity distribution along the waveguide seen in Fig. 3(b).

4. Phenomenological quantum description of the formation of an electromagnetic standing wave

A quantum description of interference is required when the illumination source emits feeble light or single photons. In these experiments, the interference pattern is formed gradually by the accumulation of numerous "clicks," i.e., individual photon-detection events [35]. We emphasize that we did not record single photon events, and we did not use a source of single photons in our experiments; however, if the experiments described in Section 2 were repeated while using feeble light, one should expect to obtain the same results after a large number of single-photon events are

recorded. In the quantum picture, the intensity where the standing wave is formed along the DLSPPW can be approximately described by the following expression [36,37]:

$$I(z) = Nh\nu|\Omega(z)|^2 \tag{6}$$

where h is Planck's constant, $\nu=c/\lambda$, N is the average number of photon that pass through the transversal section of the waveguide per unit time, and, following Feynman's approach for describing interference [28], $\Omega(z=z_o)$ is the probability amplitude per unit area (probability amplitude density) of detecting a photon passing through the transversal section of the waveguide at $z=z_o$ near the center of the waveguide. Due to Bohr's correspondence principle [24], classical and quantum descriptions should give equal results when a large number of photons are coupled to the DLSPPW; therefore, $I(z)$ in (3) and (6) should be equal, this resulting in the following proportionality relation between $|\Omega(z)|$ and $E(z)$ [37]:

$$|\Omega_E(z)| = \beta E(z), \beta = \sqrt{\frac{2}{Nh\nu}}\alpha_E \tag{7}$$

Relation (7) states that, in the classical limit, the magnitude of the probability amplitude per unit area of registering a "click" at the point $z=z_o$ is directly proportional to the amplitude of the electric field at that point. This provides a way to calculate the probability distribution of "clicks" along the DLSPPW, without having to rely on the mathematical subtleness of more elaborated quantum theories of photons [25–27]. Expression (6) provides a phenomenological definition of Ω. In this sense, satisfying relation (7) can be seen as a mandatory test for any successful quantum theory of photons. The sub index E of Ω was introduced in (7) to emphasize that Ω_E refers to the photodetection events using a common photodetector only responsive to the electric field. However, photons can be detected wherever there is electromagnetic energy in the standing wave [21–23]; therefore, a more general expression for Ω can be obtained comparing (5) and (6). This results in the following expression:

$$|\Omega_g(z)| = \sqrt{\frac{\alpha_E^2 E^2(z) + \alpha_B^2 B^2(z)}{Nh\nu}} \tag{8}$$

Expression (8) states that, in the classical limit, the most general expression of the magnitude of the probability amplitude density of registering a "click" at $z=z_o$ (using an advanced optical photodetector equally responsive to both electric and magnetic fields) depends on the amplitudes of both electric and magnetic fields at that point. In a quantum description, the uniform intensity distribution along the waveguide seen in Fig. 3(b) can be explained by the constancy of the probability per unit area, p, of finding a photon along the DLSPPW. In the classical limit, using expressions (5), (6) and (8), p can be expressed in terms of the transversal wavefunction $\psi(z,t)$ [27,38,39] of the photons in an electromagnetic standing wave in the following way:

$$p = |\Psi(z,t)|^2 = |\Omega_g(z)|^2 = \frac{2I_o}{Nh\nu} \tag{9}$$

where:

$$\Psi(z,t) = |\Omega_g(z)|e^{i\omega t} = \sqrt{\frac{\alpha_E^2 E^2(z) + \alpha_B^2 B^2(z)}{Nh\nu}}e^{i\omega t} \tag{10}$$

The complex exponential factor was included in (10) because $\psi(z,t)$ describes a stationary state [28]. The classical limit of the transversal wavefunction, $\psi(z,t)$, does not have nodes at the regions occupied by the dark fringes of the standing wave interference pattern shown in Fig. 3(a) because the magnetic field has antinodes there. The electric field does have nodes at the dark fringes but the amplitude of the transversal photon wavefunction is not exclusively determined by the electric field of the standing

wave. It is worth noting that for a plane wave $E(z)=E_o$, $B(z)=B_o$, $E_o=cB_o$ [18,30]; therefore, for a plane wave $|\Omega_g|$ is given by the following expression:

$$|\Omega_{g,p}(z)| = \sqrt{\frac{2}{Nh\nu}}\alpha_E E_o \qquad (11)$$

Consequently, in the classical limit, the amplitude of the transversal wavefunction of the photons in a electromagnetic plane wave, $\psi_p(z,t)$, is proportional to the amplitude of the electric field, i.e.:

$$\Psi_p(z,t) = \sqrt{\frac{2}{Nh\nu}}\alpha_E E_o e^{i(kz-\omega t)} \qquad (12)$$

This proportionality is not valid (see expression (10)) for the standing wave formed in the DLSPPW because the electric and magnetic fields are not equally distributed along the waveguide and do not oscillate in phase (see expressions (1) and (2)). It is worth noting that the phenomenological quantum description presented in this Section applies to the classical limit where a large number of photons are present. Even in the classical limit, light is made of photons; therefore, the quantum theory of light should be able to describe all classical optical phenomena. In the experiments described in Section 2, individual photons were not detected, and a source of single photons was not used; however, as Feynman emphasized "light is made of particles" [40]. Moreover, the quantum nature of SPP excitation has been demonstrated experimentally [41–43]. Therefore, we can predict that if the experiments described in Section 2 were repeated but using feeble light, SPP tomography will permit the detection of single photons while they are passing through the "will be" dark fringes of the standing wave interference pattern. If the experiments were done using an advanced photodetector (equally responsive to both electric and magnetic fields) a uniform illumination along the waveguide similar to the shown in Fig. 3(b) would be measured.

5. Conclusions

We presented classical and phenomenological quantum descriptions of experiments where the formation of SPP standing waves was observed using SPP tomography. Following this straightforward approach, the classical limit of the analytical expression of the transversal wavefunction of the photons in an electromagnetic standing wave was obtained. We demonstrated that SPP tomography in a quantum eraser arrangement has the remarkable capability of permitting the observation of light (photons) passing through the dark fringes of the observed standing wave interference pattern. It was shown that an electromagnetic standing wave provides a simple but effective method for producing a spatially localized pure magnetic field oscillating at light frequencies, which can be useful, for instance, for testing novel active magnetic optical metamaterials.

Acknowledgments

References

[1] Ekmel Ozbay, Science 311 (2006) 189.
[2] Yasushi Satoshi Kawata, Prabhat Verma, Nature Photonics 3 (2009) 388.
[3] M.T. Hill, M. Marell, E.S.P. Leong, B. Smalbrugge, Y. Zhu, M. Sun, P.J. van Veldhoven, E.J. Geluk, F. Karouta, Y.S. Oei, R. Nötzel, C.Z. Ning, M.K. Smit, Optics Express 17 (2009) 11107.
[4] H. Raether, Surface Plasmons on Smooth and Rough Surfaces and on Gratings, Springer-Verlag, Berlin, 1988.
[5] L. Grave de Peralta, R. Lopez-Boada, A. Ruiz-Columbie, S. Park, A.A. Bernussi, Journal of Applied Physics 109 (2011) 023101.
[6] A. Houk, R. Lopez-Boada, A. Ruiz-Columbie, S. Park, A.A. Bernussi, L. Grave de Peralta, Journal of Applied Physics 109 (2011) 119901.
[7] C.J. Regan, A. Krishnan, R. Lopez-Boada, L. Grave de Peralta, A.A. Bernussi, Applied Physics Letters 98 (2011) 151113.
[8] S.P. Frisbie, C. Chesnutt, M.E. Holtz, A. Krishnan, L. Grave de Peralta, A.A. Bernussi, IEEE Photonics Journal 1 (2009) 153.
[9] A. Drezet, A. Hohenau, D. Koller, A. Stepanov, H. Ditlbacher, B. Steinberger, F.R. Aussenegg, A. Leitner, J.R. Krenn, Materials Science and Engineering B 149 (2008) 220.
[10] B. Hecht, H. Bielefeldt, L. Novotny, Y. Inouye, H. Ditlbacher, D.W. Pohl, Physics Review Letters 77 (1996) 1889.
[11] J. Ajimo, C.J. Regan, A.C. Bernussi, S. Park, R. Lopez-Boada, A.A. Bernussi, L. Grave de Peralta, Optics Communications 284 (2011) 4752.
[12] J. Ajimo, M. Marchante, A. Krishnan, A.A. Bernussi, L. Grave de Peralta, Journal of Applied Physics 108 (2010) 063110.
[13] L. Grave de Peralta, Journal of the Optical Society of America B, Optical physics 27 (2010) 1513.
[14] A. Drezet, A.L. Stepanov, A. Hohenau, B. Steinberger, N. Galler, H. Ditlbacher, A. Leitner, F.R. Aussenegg, J.R. Krenn, M.U. Gonzalez, J.-C. Webber, Europhysics Letters 74 (4) (2006) 693.
[15] J. Grandidier, S. Massenot, G. Colas des Francs, A. Bouhelier, J.-C. Weeber, L. Markey, A. Dereux, J. Renger, M.U. González, R. Quidant, Physical Review B 78 (2008) 245419.
[16] A. Krishnan, C.J. Regan, L. Grave de Peralta, A.A. Bernussi, Applied Physics Letters 97 (2010) 231110.
[17] M. Born, E. Wolf, Principles of Optics, Pergamon Press, New York, 1964.
[18] F.L. Pedrotti, L.S. Pedrotti, L.S. Pedrotti, Introduction to Optics, Pearson Prentice Hall, New Jersey, 2007.
[19] Optical S. Linden, C. Enkrich, G. Dolling, M.W. Klein, J. Zhou, T. Koschny, C.M. Soukoulis, S. Burger, F. Schmidt, M. Wegener, IEEE Journal of Selected Topics in Quantum Electronics 12 (2006) 1097.
[20] N.I. Landy, S. Sajuyigbe, J.J. Mock, D.R. Smith, W.J. Padilla, Physical Review Letters 100 (2008) 207402.
[21] M. Burresi, T. Kampfrath, D. van Oosten, J.C. Prangsma, B.S. Song, S. Noda, L. Kuipers, Physical Review Letters 105 (2010) 123901.
[22] S. Vignolini, F. Intonti, F. Riboli, L. Balet, L.H. Li, M. Francardi, A. Gerardino, A. Fiore, D.S. Wiersma, M. Gurioli, Physical Review Letters 105 (2010) 123902.
[23] K. Münter, R. Pape, M. Spitzer, J. Glimm, Traceable calibration on magnetic field transfer sensors up to 1 GHz in a radiated standing wave pattern, in: Proceeding of the 15th International Zurich Symposium and Technical Exhibition on Electromagnetic Compatibility, EMC, Zurich, 2003.
[24] B.L. Van Der Waerden, Sources of Quantum Mechanics, in: G. Holton (Ed.), Dover, New York, 1967.
[25] M.O. Scully, M.S. Zubairy, Quantum Optics, Cambridge University Press, Cambridge, 1997.
[26] R.P. Feynman, A.R. Hibbs, Quantum Mechanics and Path Integrals, MacGraw-Hill, New York, 1965.
[27] B.J. Smith, M.G. Raymer, New Journal of Physics 9 (2007) 414.
[28] R.P. Feynman, R.B. Leighton, M. Sands, The Feynman Lectures on Physics, vol II, Addison-Wesley, Massachusetts, 1965.
[29] S.P. Frisbie, C. Chesnutt, J. Ajimo, A.A. Bernussi, L. Grave de Peralta, Optics Communications 283 (2010) 5255.
[30] E. Hetcht, Optics, Fourth Edition, Pearson-Addison Wesley, New York, 2002.
[31] W. Holladay, Physics Letters A 183 (1993) 280.
[32] A. Passian, A. Wig, A.L. Lereu, P.G. Evans, F. Mariaudeau, T. Thundat, T.L. Ferrell, Ultramicroscopy 100 (2004) 429.
[33] J.-C. Weeber, J.R. Krenn, A. Dereux, B. Lamprecht, Y. Lacroute, J.P. Goudonnet, Physical Review B **64** (2001) 045411.
[34] J.W. Goodman, Introduction to Fourier Optics, McGraw-Hill, New York, 1968.
[35] A. Zeilinger, G. Weihs, T. Jennewein, M. Asspeimeyer, Nature 433 (2005) 230.
[36] D. Bohm, Quantum Theory, in: N.J. Englewood Cliffs (Ed.), Prentice Hall, 1951.
[37] L. Grave de Peralta, Journal of Applied Physics 108 (2010) 103110.
[38] J.S. Lundeen, B. Sutherland, A. Patel, C. Stewart, C. Bamber, Nature 474 (2011) 188.
[39] I. Bialynicki-Birula, Photon wave function, in: E. Wolf (Ed.), Progress in Optics, vol. XXXVI, Elsevier, Amsterdam, 1996, p. 245.
[40] R.P. Feynman, QED: The Strange Theory of Light and Matter, Princeton University Press, Princeton, 1985.
[41] E. Altewischer, M.P. van Exter, J.P. Woerdman, Nature 418 (2002) 304.
[42] A.V. Akimov, A. Mukherjee, C.L. Yu, D.E. Chang, A.S. Zibrov, P.R. Hemmer, H. Park, M.D. Lukin, Nature 450 (2007) 402.
[43] G. Di Martino, Y. Sonnefraud, S. Kéna-Cohen, M. Tame, S.K. Özdemir, M.S. Kim, S.A. Maier, Quantum statistics of surface plasmon polariton in metallic stripe waveguides, Nano Letters 12 (2012) 2504.